**C**urrent **A**pplied **S**cience and **T**echnology e-ISSN: 2586-9396

Curr. Appl. Sci. Technol. ….., Vol... (No...), e0263969

## *Research article*

# Influence of Dragon Fruit Peels on the Synthesis of Antibacterial Nano Zinc Oxide (Nano-ZnO) via Green Synthesis Method

**Natchayaporn Sakulpeeb[1], Wantana Koetniyom[2,3], Sutee Chutipaijit[1], Sakon Rahong[1], Navaphun Kayunkid[1], Adirek Rangkasikorn[1], Supamas Wirunchit[1]*and Jiti Nukaew[1]**

*[1]College of Materials Innovation and Technology (CMIT), King Mongkut's Institute of Technology Ladkrabang, Ladkrabang, Bangkok 10520, Thailand*
*[2]Department of Industrial Physics and Medical Instrumentation, Faculty of Applied Science, King Mongkut's University of Technology North Bangkok, Bangkok 10800, Thailand*
*[3]Lasers and Optics Research Center (LANDOS), King Mongkut's University of Technology North Bangkok, Bangkok 10800, Thailand*

Received: 10 July 2024, Revised: 20 November 2024, Accepted: 27 November 2024, Published: 10 October 2025

## Abstract

This research focused on adding value to dragon fruit peel waste by utilizing it in the synthesis of antibacterial nano zinc oxide (Nano-ZnO) through a green synthesis process. In this study, all the dragon fruit peels were extracted using the solvent extraction technique with three different solvents (deionized water, ethanol, and methanol) for 1, 2, 3, 4, and 5 h, respectively. The amount of flavonoids from the extract was determined using UV-Vis spectrophotometer to obtain the optimum extraction time, which was 4 h for DI water as the solvent. Moreover, antibacterial Nano-ZnO was synthesized successfully by a green synthesis process using zinc nitrate $Zn(NO_3)_2$ and the extracts. The molecular vibrations as well as the crystal structure and morphology were investigated by Fourier transform infrared spectroscopy (FT-IR), Raman spectroscopy (Raman), X-ray diffraction (XRD), and field emission scanning electron microscopy (FE-SEM), respectively. Additionally, the antibacterial efficacy of the nano-zinc oxide samples was evaluated using disc diffusion method. Gram-positive bacteria (*Staphylococcus aureus*) and Gram-negative bacteria (*Escherichia coli*) were the test agents. The research shows that the X-ray diffraction patterns of all synthesized ZnO nanoparticles (NPs) exhibited a wurtzite (hexagonal) crystal structure. FT-IR spectroscopy confirmed the presence of Zn-O stretching vibrations at approximately 500 $cm^{-1}$. Furthermore, the FE-SEM reveals that ZnO-yellow particles displayed spherical morphologies with an average particle size of 145 nm. At the same time, ZnO-White and ZnO-Red nanoparticles exhibited a combination of rod-like and elliptical morphologies, with average particle sizes of 168 nm and 321 nm, respectively. In addition, the antibacterial activity demonstrates effective inhibition against *S. aureus* and *E. coli* in all three ZnO nanoparticle conditions.

**Keywords:** green synthesis; dragon fruit peels extraction; nano zinc oxide; antibacterial activity

*Corresponding author: E-mail: supamas.wirun@gmail.com
https://doi.org/10.55003/cast.2025.263969

## 1. Introduction

In recent years, ZnO NPs have attracted significant attention from researchers due to their unique optical properties, leading to their widespread application in various fields including electronics, textiles, cosmetics, and biology (Rahman et al., 2022). ZnO NPs can be synthesized using different methods including chemical and physical approaches. However, green synthesis has emerged as a promising alternative due to its safety, environmental friendliness, reduced researcher exposure to hazards (Mendes et al., 2024), sustainability, and cost-effectiveness (Naiel et al., 2022).

Green synthesis involves synthesizing nanostructured materials using plant extracts, microorganisms, bacteria, and other natural resources as reducing agents instead of conventional chemical reductants. Consequently, various plant parts have been employed for ZnO NP synthesis because plant extracts contain phytochemicals such as flavonoids, phenols, saponins, alkaloids, tannins, and terpenes, which act as both reducing and capping, or stabilizing agents (Loganathan et al., 2021; Mahmoud et al., 2022).

Dragon fruit (*Hylocereus* spp.) is a tropical fruit belonging to the genus *Hylocereus* and the Cactaceae family. It originated in the West Indies and Latin America (Aminuzzaman et al., 2019). Vietnam was the first to introduce it to Southeast Asia, and it has since become an economically important crop in Thailand. The fruit contains tiny black seeds and has a skin with different colors depending on the variety. The most common varieties are *Hylocereus polyrhizus* (red flesh with red skin), *Hylocereus megalanthus* (white flesh with yellow skin), and *Hylocereus undatus* (white flesh with red skin). Dragon fruit flesh is highly popular among consumers due to its nutritional and medicinal benefits. Moreover, the discarded peel can add value, as it contains betacyanin, anthocyanins, and other flavonoids, making it a source of antioxidants, anti-inflammatory agents, and reducing agents (Khoo et al., 2022).

## 2. Materials and Methods

This research study focused on the valorization of dragon fruit peels from three varieties into antibacterial zinc oxide nanomaterials via a green synthesis process. Schematic diagram of all steps in this research is presented in Figure 1. All analyses were described as follows.

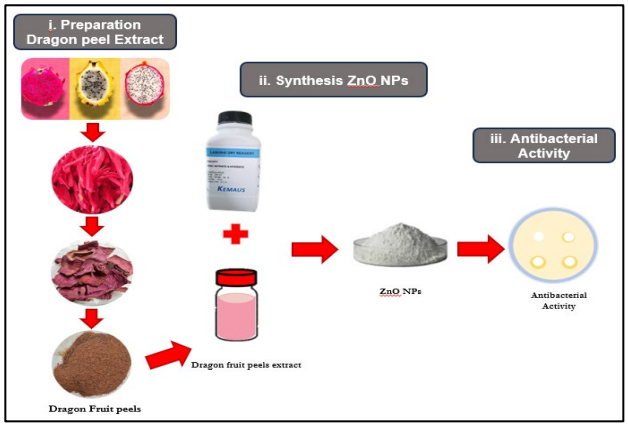


**Figure 1.** Schematic diagram of all steps in this research

## 2.1 Dragon fruit peel waste

Dragon fruit peel wastes, i.e. *Hylocereus polyrhizus* (Red), *H. megalantus* (Yellow), and *H. undatus* (White), were collected from industrial factories and washed with tap water to remove impurities. The peels were then rinsed with deionized water and dried in an oven at 60°C for 12-24 h or until completely dry. The dried peels were ground into fine powder using a blender and stored for further extraction. Zinc nitrate 6-hydrate ($Zn(NO_3)_2.6H_2O$) of laboratory grade (KemAus, Australia) was used as the zinc precursor.

## 2.2 Extraction of flavonoids from dragon fruit peel

Two grams of each prepared dragon fruit peel powder were mixed with 100 mL of different solvents (deionized water, ethanol, and methanol) in Erlenmeyer flasks. The mixtures were shaken for various durations (1, 2, 3, 4, and 5 h). After each shaking period, the Erlenmeyer flasks were heated in a water bath at 60°C for 1 h. The solutions were then filtered using Whatman No. 1 filter paper. Finally, the total flavonoid content of each extract was determined using a Thermo Scientific Orion AquaMate 7000 Vis spectrophotometer by measuring the absorbance at 374 nm ($A_{374}$). The total flavonoid content was then calculated using equation (1) and expressed as milligrams of Quercetin equivalent per gram of dry fruit peel (mg/g) (Pedro et al., 2016).

$$\text{Total flavonoids (TF)} = \frac{A_{374nm} \times dilution\ factor}{76.6} \quad (1)$$

## 2.3 Green synthesis of ZnO NPs

In this step, different dragon fruit peel extracts, extracted using deionized water as the solvent, were used as reducing agents for synthesizing zinc oxide nanoparticles. Two grams of zinc nitrate were mixed with the extracts in different ratios (5, 10, 15, 20, 25, and 30 mL) in a 50 ml beaker. The mixture was then stirred at 300 rpm for 1 h and placed in a water bath at 60°C for 1 h. The solution was dried in an oven at 60°C. Finally, the samples were calcined at 500°C for 4 h. The resulting zinc oxide nanoparticles were referred to as ZnO-Red, ZnO-Yellow, and ZnO-White.

## 2.4 Analysis of ZnO NPs

The crystallinity of the synthesized ZnO nanoparticles was analyzed using X-ray diffraction (XRD) with a Smart lab diffractometer (Rigaku) to confirm their identity. The Raman spectra were recorded using a DXR Raman spectrometer (Thermo Scientific) and FTIR spectroscopy was employed to identify the functional groups on the nanoparticles. The morphology of the nanoparticles was examined using a field emission scanning electron microscope (FE-SEM) (Apreo S-Thermo Fisher Scientific).

## 2.5 Antimicrobial activity assay

The antibacterial activity of the synthesized zinc oxide nanoparticles was evaluated using the disc diffusion method (Santhoshkumar et al., 2014). The nanoparticles were dispersed in water to obtain a 0.3 mg/mL concentration. Aliquots of 20 µL of the nanoparticle suspension were dropped onto sterile filter paper discs (6 mm diameter) placed on the surface of agar plates previously inoculated with the test bacteria (*Staphylococcus aureus*

and *Escherichia coli*). The plates were incubated at 37°C for 24 h. The inhibition zones around the discs were measured and recorded and the larger the inhibition zone, the greater the antibacterial activity of the nanoparticles.

## 3. Results and Discussion

### 3.1 Preparation of extract and synthesis of zinc oxide nanoparticles

Figure 2 shows the effect of each dragon fruit extract. Deionized water was found to be the most effective solvent for extracting flavonoids, with the highest yield obtained after 4 h of extraction. This was likely due to the neutral pH of deionized water, which promoted the solubility of flavonoids and minimizes chemical reactions that could degrade them (Wyrostek & Kowalski, 2021).

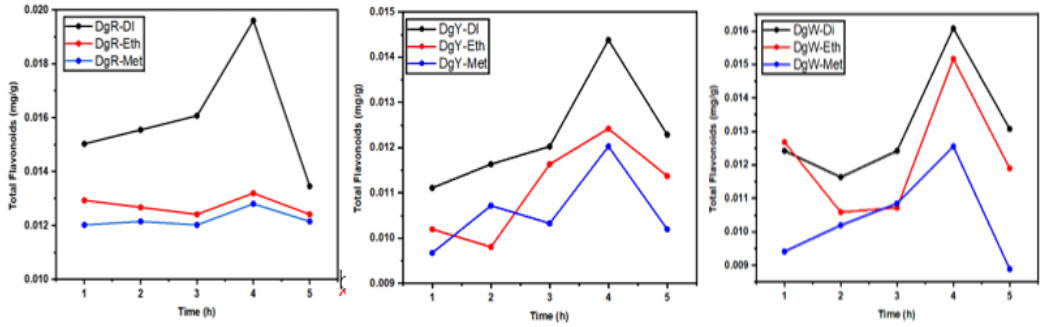


**Figure 2.** Effect of extraction time on the flavonoid content of dragon fruit extracts (a) Red dragon fruit extract (b) Yellow dragon fruit extract (c) White dragon fruit extract
DgR-DI = Extract from red dragon fruit using deionized water as the solvent,
DgR-Eth = Extract from red dragon fruit using ethanol as the solvent,
DgR-Met = Extract from red dragon fruit using methanol as the solvent
DgY-DI = Extract from yellow dragon fruit using deionized water as the solvent,
DgY-Eth = Extract from yellow dragon fruit using ethanol as the solvent,
DgY-Met = Extract from yellow dragon fruit using methanol as the solvent
DgW-DI = Extract from white dragon fruit using deionized water as the solvent,
DgW-Eth = Extract from white dragon fruit using ethanol as the solvent,
DgW-Met = Extract from white dragon fruit using methanol as the solvent

Zinc oxide nanoparticles (ZnO NPs) were synthesized using the obtained extracts as reducing agents. Different volumes of the extract (5, 15, 20, 25, and 30 mL) were used, and the percent yield was calculated to determine the optimal extract volume relative to the zinc nitrate precursor. It was found that at least 25 mL of dragon fruit peel extract was required for ZnO NP synthesis under all conditions, as shown in Figure 3. The reaction between the extract and zinc nitrate can be represented by equation (2):

$$Zn(NO_3)_2.6H_2O_{(solid)} + \text{flavonoid extract}_{(liquid)} \rightarrow ZnO + \text{organic product} \quad (2)$$

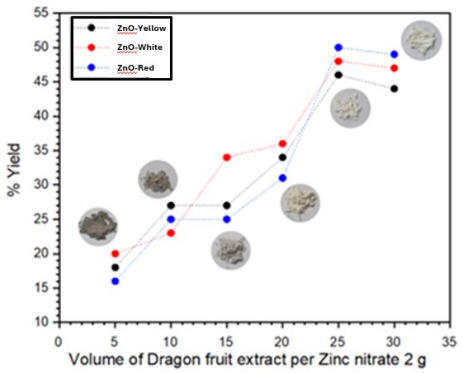


**Figure 3.** The percent yield of zinc oxide nanoparticles (ZnO NPs) synthesized using different volumes of dragon fruit peel extract.
ZnO-Yellow = zinc oxide synthesized using yellow dragon fruit peel extract,
ZnO-White = zinc oxide synthesized using white dragon fruit peel extract,
ZnO-Red = zinc oxide synthesized using red dragon fruit peel extract

## 3.2 Characterization of zinc oxide nanoparticles

The crystallites of the ZnO NPs synthesized using different dragon fruit peel extracts were analyzed with X-ray diffractometer (XRD), as shown in Figure 4a. The X-ray diffraction (XRD) patterns displayed the (100), (002), (101), (102), (110), (103), (200), (112), (201), (004), and (202) hexagonal wurtzite crystal planes of ZnO, observed at 2θ angles of 36.2°, 31.7°, 34.4°, 36.9°, 43.2°, 56.9°, 62.9°, 69.1°, 72.6°, and 76.3°, respectively. All the diffraction patterns corresponded to the JCPDS file No. 36-1451 of wurtzite-type ZnO (Thi et al., 2020). The average crystallite size was calculated using the Scherrer equation: $D = (0.9 \times \lambda)/(\beta \times \cos\theta)$ (Å), where λ is the wavelength of Cu Kα radiation (1.5406 Å), β is the full width at half maximum (rad), and θ is the diffraction angle (degrees) (Sharma et al., 2012). The average crystallite sizes for the ZnO NPs synthesized using the red, yellow, and white dragon fruit peel extracts were 207 nm, 266 nm, and 188 nm, respectively.

The Raman-active modes of the ZnO wurtzite crystal was shown in the Raman spectra (Figure 4b) to confirm the hexagonal wurtzite crystal structure of the synthesized ZnO NPs (Sharma et al., 2012). Wurtzite-type ZnO, with two formula units per primitive cell, belongs to the space group P63mc. The zone center optical phonons can be classified according to the following irreducible representation: $\Gamma opt = A_1 + E_1 + 2E_2 + 2B_1$, where $A_1$ and $E_1$ are polar modes, $B_1$ modes are silent and both Raman and infrared active, while $E_2$ modes ($E_2^{low}$ and $E_2^{high}$) are Raman active only and nonpolar. The $E_2^{low}$ peak appears at approximately 320 $cm^{-1}$, which matches well with the lattice vibrations of ZnO. The $E_2^{high}$ peak is observed at 437 $cm^{-1}$, which is primarily associated with the vibrations of oxygen atoms (Šćepanović et al., 2010; Sharma et al., 2012). Additionally, a peak around 1050 $cm^{-1}$ is characteristic of annealed ZnO samples, as previously observed in the Raman spectra of annealed samples prepared from ZnO powder ground in a zirconia vial (Vojisavljevic et al., 2008).

Fourier transform infrared (FTIR) spectra were used to analyze the composition of the synthesized ZnO nanoparticles. Figure 4c shows the FTIR spectra of the ZnO NPs. The characteristic Zn-O stretching mode is observed at 500 $cm^{-1}$, while the symmetric stretching vibration of hydroxyl groups appears at 3400 $cm^{-1}$.

The morphology of the ZnO nanoparticles synthesized using different dragon fruit peel extracts is shown in Figure 5. As can be seen, the synthesized nanoparticles are uniformly distributed and have a smooth surface. ZnO-Yellow exhibits spherical morphologies (Bhuiyan & Mamur, 2021), with 145 nm particle sizes. In contrast, ZnO-White and ZnO-Red nanoparticles exhibit a combination of rod-like and elliptical morphologies, with a particle size of 168 and 321 nm, respectively (Figures 5b and 5c). The shorter nanorod length of ZnO-White observed in Figure 5b is likely due to the lower flavonoid content in the white dragon fruit extract (Tang et al., 2021). The reduced flavonoid concentration may have inhibited the growth of ZnO nanorods.

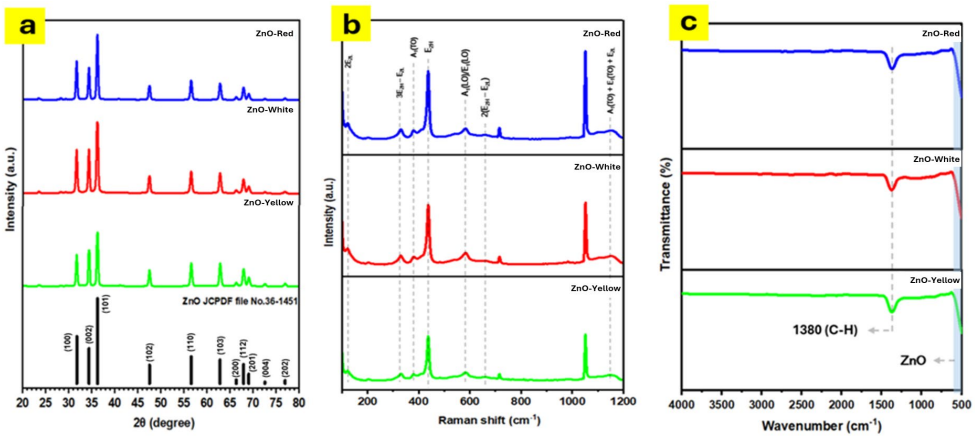


**Figure 4.** Structural characterization of ZnO NPs: (a) XRD (b) Raman (c) FTIR

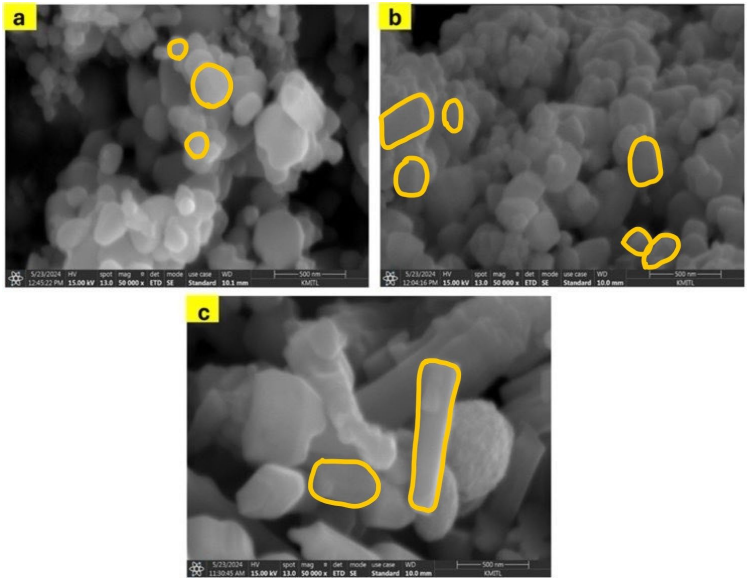


**Figure 5.** FE-SEM images of ZnO synthesized with different dragon fruit peels at magnification of 50,000X; (a) ZnO-Yellow (b) ZnO-White (c) ZnO-Red

### 3.3 Antibacterial activity

The antibacterial activity of ZnO-Yellow, ZnO-White, and ZnO-Red against Gram-negative bacterium (*E. coli*) and Gram-positive bacterium (*S. aureus*) was evaluated. All three ZnO samples exhibited antibacterial activity against *E. coli* and *S. aureus*. However, ZnO-White showed the highest antibacterial activity, as evidenced by the largest clear zones of 2.73 cm for *E. coli* and 1.27 cm for *S. aureus*, as shown in Figure 6c. This enhanced activity of ZnO-White may be attributed to its superior ability to disrupt the bacterial cell membrane. With their thinner cell walls, Gram-negative bacteria are generally more susceptible to ZnO nanoparticles than Gram-positive bacteria. The mechanism that causes cell death occurs when zinc oxide nanoparticles are ionized, diffuse into cells, and react with bacterial cell walls. This interaction involves the following mechanisms: (1) the production of ROS, including $OH^-$ (hydroxyl radical) and $O_2^{-2}$ (peroxide) from the ionization of ZnO. These ROS induce cell membrane disruption and DNA damage, ultimately leading to cell death (2) the ionization of zinc oxide nanoparticles into $Zn^{2+}$ ions, which react with bacterial cells, especially the cell membrane, cytoplasm, and nucleic acids, causing cell lysis and resulting in bacterial cell death, and (3) direct interactions between zinc oxide nanoparticles and bacterial cell membranes through electrostatic forces that damage the plasma membrane and cause a leakage of intracellular components (Murali et al., 2021; Gomaa, 2022).

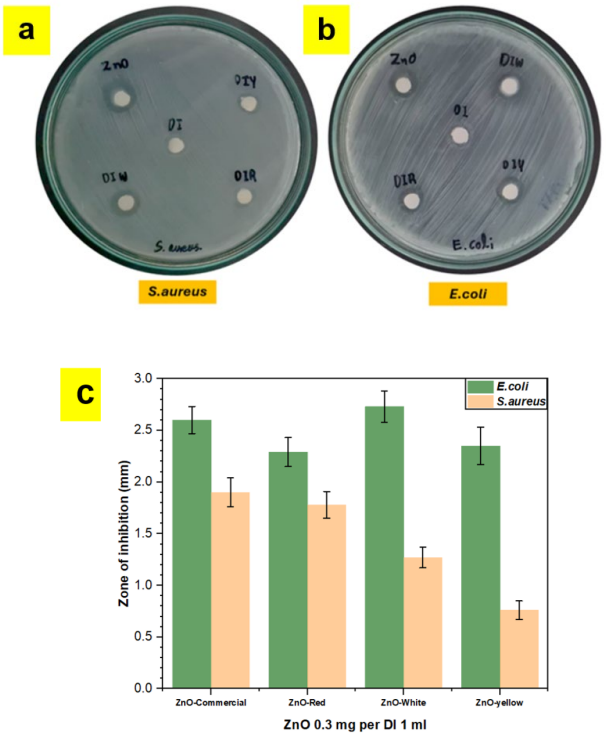


**Figure 6.** The inhibition zones of *S. aureus* (a) and *E. coli* (b) by ZnO nanoparticles synthesized using different dragon fruit peels and comparison of inhibition zone (c)

## 4. Conclusions

The extracts from three different dragon fruit varieties (white, red, and yellow) as reducing agents in the green synthesis of zinc oxide nanoparticles (ZnO NPs) were investigated in this study. Deionized water was found to extract the highest amount of flavonoids. All three dragon fruit extracts were successfully used to synthesize ZnO NPs. The ZnO NPs synthesized using white dragon fruit extract exhibited the smallest crystal size (188 nm) as confirmed by X-ray diffraction (XRD) analysis. Field emission scanning electron microscopy (FE-SEM) images revealed that the ZnO NPs synthesized using white dragon fruit extract also had the smallest particle size (145 nm). Finally, antibacterial activity assays demonstrated that the ZnO NPs synthesized using all three dragon fruit extracts effectively inhibited both *E. coli* and *S. aureus.*

## 5. Acknowledgements

Thanks to Nanotechnology and Material Analytical Instrument Service Unit (NMIS), School of Integrated Innovative Technology, King Mongkut's Institute of Technology Ladkrabang and Department of Nanoscience and Nanotechnology, School of Integrated Innovative Technology (SIITec), King Mongkut's Institute of Technology Ladkrabang (KMITL).

## 6. Authors' Contributions

Natchayaporn Sakulpeeb initiated and formulated the research hypothesis, designed the experiment, developed and tested the measurement tools, collected and analyzed the data, interpreted the results, and contributed to the writing of the manuscript; Wantana Koetniyom was involved in the interpretation and critical discussion of the experimental findings, in comparison with established conclusions, knowledge, or theories; Sutee Chutipaijit contributed to the discussion of the microbiology experimental results, comparing them with established conclusions, knowledge, and theories; Sakon Rahong participated in a critical discussion of the experimental results regarding the physical and morphological relationships of the synthesized materials, comparing them with established conclusions, knowledge, or existing theories; Navaphun Kayunkid contributed to a critical analysis of the experimental results in crystallography, comparing them with established conclusions, knowledge, or theories; Adirek Rangkasikorn critically analyzed the experimental results concerning the physical properties of the synthesized material, and subsequently compared them with pre-existing conclusions, established knowledge, or theoretical frameworks; Supamas Wirunchit contributed to the experimental design, data analysis, results interpretation, critical review of the findings, and comparison with existing knowledge and theories; Jiti Nukaew reviewed and evaluated the research findings

## 7. Conflicts of Interest

The authors declare that they have no conflicts of interest concerning the research, authorship, and/or publication of this article.

**ORCID**

Supamas Wirunchit https://orcid.org/0009-0000-3691-012

## References

Aminuzzaman, M., Ng, P. S., Goh, W.-S., Ogawa, S., & Watanabe, A. (2019). Value-adding to dragon fruit (*Hylocereus polyrhizus*) peel biowaste: green synthesis of ZnO nanoparticles and their characterization. *Inorganic and Nano-Metal Chemistry*, 49(11), 401-411. https://doi.org/10.1080/24701556.2019.1661464

Bhuiyan, M. R. A., & Mamur, H. (2021). A brief review of the synthesis of ZnO Nanoparticles for biomedical applications. *Iranian Journal of Materials Science and Engineering*, 18(3), 1-27.

Gomaa, E. Z. (2022). Microbial mediated synthesis of zinc oxide nanoparticles, characterization and multifaceted applications. *Journal of Inorganic and Organometallic Polymers and Material*s, 32, 414-4132. https://doi.org/10.1007/s10904-022-02406-w

Khoo, H. E., He, X., Tang, Y., Li, Z., Li, C., Zeng, Y., Tang, J., & Sun, J. (2022). Betacyanins and anthocyanins in pulp and peel of red pitaya (*Hylocereus polyrhizus* cv. Jindu), inhibition of oxidative stress, lipid reducing, and cytotoxic effects. *Frontiers in Nutrition*, 9, 894438. https://doi.org/10.3389/fnut.2022.894438

Loganathan, S., Shivakumar, M. S., Karthi, S., Nathan, S. S., & Selvam, K. (2021). Metal oxide nanoparticle synthesis (ZnO-NPs) of *Knoxia sumatrensis* (Retz.) DC. Aqueous leaf extract and It's evaluation of their antioxidant, anti-proliferative and larvicidal activities. *Toxicology Reports*, 8, 64-72. https://doi.org/10.1016/j.toxrep.2020.12.018

Mahmoud, A. E. D., El-Maghrabi, N., Hosny, M., & Fawzy, M. (2022). Biogenic synthesis of reduced graphene oxide from *Ziziphus spina-christi* (Christ's thorn jujube) extracts for catalytic, antimicrobial, and antioxidant potentialities. *Environmental Science and Pollution Research*, 29, 89772-89787. https://doi.org/10.1007/s11356-022-21871-x

Mendes, A. R., Granadeiro, C. M., Leite, A., Pereira, E., Teixeira, P., & Poças, F. (2024). Optimizing antimicrobial efficacy: Investigating the impact of zinc oxide nanoparticle shape and size. *Nanomaterials*, 14(7), Article 638. https://doi.org/10.3390/nano14070638

Murali, M., Kalegowda, N., Gowtham, H. G., Ansari, M. A., Alomary, M. N., Alghamdi, S., Shilpa, N., Singh, S. B., Thriveni, M. C., Aiyaz, M., Angaswamy, N., Lakshmidevi, N., Adil, S. F., Hatshan, M. R., & Amruthesh, K. N. (2021). Plant-mediated zinc oxide nanoparticles: advances in the new millennium towards understanding their therapeutic role in biomedical applications. *Pharmaceutics*, 13(10), Article 1662. https://doi.org/10.3390/pharmaceutics13101662

Naiel, B., Fawzy, M., Halmy, M. W. A., & Mahmoud, A. E. D. (2022). Green synthesis of zinc oxide nanoparticles using sea lavender (*Limonium pruinosum* L. Chaz.) extract: characterization, evaluation of anti-skin cancer, antimicrobial and antioxidant potentials. *Scientific Reports*, 12, Article 20370. https://doi.org/10.1038/s41598-022-24805-2

Pedro, A. C., Granato, D., & Rosso, N. D. (2016). Extraction of anthocyanins and polyphenols from black rice (Oryza sativa L.) by modeling and assessing their reversibility and stability. *Food Chemistry*, 191, 12-20. https://doi.org/10.1016/j.foodchem.2015.02.045

Rahman, F., Majed Patwary, M. A., Bakar Siddique, M. A., Bashar, M. S., Haque, M. A., Akter, B., Rashid, R., Haque, M. A., & Royhan Uddin, A. K. M. (2022). Green synthesis of zinc oxide nanoparticles using *Cocos nucifera* leaf extract: characterization, antimicrobial, antioxidant and photocatalytic activity. *Royal Society Open Science*, 9(11), Article 220858. https://doi.org/10.1098/rsos.220858

Santhoshkumar, T., Rahuman, A. A., Jayaseelan, C., Rajakumar, G., Marimuthu, S., Kirthi, A. V., Velayutham, K., Thomas, J., Venkatesan, J., & Kim, S.-K. (2014). Green synthesis of titanium dioxide nanoparticles using Psidium guajava extract and its

antibacterial and antioxidant properties. *Asian Pacific Journal of Tropical Medicine*, *7*(12), 968-976. https://doi.org/10.1016/S1995-7645(14)60171-1

Šćepanović, M., Grujić-Brojčin, M., Vojisavljevic, K., Bernik, S., & Srećković, T. (2010). Raman study of structural disorder in ZnO nanopowders. *Journal of Raman Spectroscopy*, 41, 914-921. https://doi.org/10.1002/jrs.2546

Sharma, A., Singh, B. P., Dhar, S., Gondorf, A., & Spasova, M. (2012). Effect of surface groups on the luminescence property of ZnO nanoparticles synthesized by sol–gel route. *Surface Science*, 606(3-4), L13-L17. https://doi.org/10.1016/j.susc.2011.09.006

Tang, W., Li, W., Yang, Y., Lin, X., Wang, L., Li, C., & Yang, R. (2021). Phenolic compounds profile and antioxidant capacity of pitahaya fruit peel from two red-skinned species (*Hylocereus polyrhizus* and *Hylocereus undatus*). *Foods*, 10(6), Article 1183. https://doi.org/10.3390/foods10061183

Thi, T. U. D., Nguyen, T. T., Thi, Y. D., Thi. K. H. T., Phan, B. T., & Pham, K. N. (2020). Green synthesis of ZnO nanoparticles using orange fruit peel extract for antibacterial activities. *RSC Advances*, 10(40), 23899-23907. https://doi.org/10.1039/D0RA04926C

Vojisavljevic, K., Šćepanović, M., Sreckovic, T., Grujić-Brojčin, M., Brankovic, Z., & Brankovic, G. (2008). Structural characterization of mechanically milled ZnO: Influence of zirconia milling media. *Journal of Physics: Condensed Matter*, 20, Article 475202. https://doi.org/10.1088/0953-8984/20/47/475202

Wyrostek, J., & Kowalski, R. (2021). The effect of water mineralization on the extraction of active compounds from selected herbs and on the antioxidant properties of the obtained brews. *Foods*, 10(6), Article 1227. https://doi.org/10.3390/foods10061227